Acta Cryst. (1980). B**36**, 264–271

The Geometry of Calcium–Water Interactions in Crystalline Hydrates

BY HOWARD EINSPAHR AND CHARLES E. BUGG

Institute of Dental Research and Department of Biochemisty, University of Alabama in Birmingham, University Station, Birmingham, Alabama 35294, *USA*

(*Received* 24 *May* 1979; *accepted* 4 *September* 1979)

Abstract

The geometries of some 150 examples of calcium–water interactions in crystalline hydrates are examined. In the majority of examples, the calcium ion is found to lie near the plane bisecting the water molecule, although θ, the angle between the Ca--O vector and the water-dipole vector, covers a broad range. There is an apparent correlation between R, the Ca--O distance, and θ; examples with shorter R tend to show calcium ions more nearly colinear with the water dipole. These findings indicate that calcium–water interactions involve factors that impose significant constraints on the geometries of the resultant complexes.

Introduction

The structural chemistry of calcium, and of other alkaline-earth and alkali-metal ions, has been a subject of increasing interest during the past several years. It is generally accepted that interactions of these metal ions with various ligands are largely due to electrostatic factors, and that the major electrostatic terms are of the ion–ion, Coulomb type when the ligands are negatively charged and of the ion–dipole type when the ligands are uncharged. However, within the framework of a qualitative electrostatic model, it is not clear what geometrical arrangements would be expected for particular types of ligands. One might reasonably expect that factors such as the structural or electronic configurations of a ligand could restrict the range of geometries exhibited by complexes with these cations. For example, a number of authors have discussed applications of lone-pair descriptions of the electron distribution about the water molecule to analyze the water-binding patterns in a variety of crystalline hydrates that contain metal cations, including alkaline-earth and alkali-metal ions (Chidambaram, Sequeira & Sikka, 1964; Hamilton & Ibers, 1968; Ferraris & Franchini-Angela, 1972; Falk & Knop, 1973; Friedman & Lewis, 1976). In addition, more sophisticated quantum-mechanical calculations have predicted minimum-energy configurations for various cation–ligand complexes (Diercksen, Kraemer & Roos, 1975; Kollman & Kuntz, 1972; Perahia, Pullman & Pullman, 1976).

We are in the process of compiling crystallographic data on calcium interactions with certain specific types of ligands in the hope that we may be able to identify geometrical features of a general nature that would aid in the understanding of the structural chemistry of calcium. In this paper, we present the results of our initial study, an analysis of calcium–water interactions in crystal structures of hydrated calcium salts.

Experimental

Criteria for selecting calcium–water examples

149 examples of calcium-bound water molecules from 62 different crystal structures are included in this analysis. Only water molecules for which H-atom positions have been experimentally determined are considered. The reliability of these H-atom coordinates varies considerably; most are from X-ray diffraction studies, although about 10% are from neutron diffraction studies. Many of the H-atom positions have been refined by least squares, but a large number have been simply assigned from Fourier maps. It is likely that many of these H coordinates have significant errors, possibly ranging up to 0·6 Å. For the purpose of our survey, we have assumed that such errors are randomly distributed except that those H atoms from X-ray diffraction studies may have been systematically displaced toward the O atoms of the water molecules. We have excluded those examples that contain obviously large errors in H-atom positions by discarding all examples (five) of water molecules that display Ca···H contacts significantly shorter than corresponding Ca--O distances and that display Ca--O–H angles smaller than 75° (Baur, 1972, 1973). We encountered three examples of water molecules that were disordered, resulting in two alternative configurations that were unrelated by crystallographic symmetry; in these cases, both configurations are included among the final set of calcium–water interactions. Histograms of the O–H distances and of the H–O–H angles for the 143 crystallo-

0567-7408/80/020264-08$01.00

graphically distinct water molecules suggest that these quantities are normally distributed about mean values of 0·87 (13) Å and 108 (10)°, respectively. Table 1 lists the crystal structures that have contributed calcium–water examples for this analysis.

Parameters describing the geometry of calcium–water interactions

A convenient reference direction with which to describe the distribution of orientations that water molecules assume relative to Ca ions is the water dipole-moment vector. In this study, we assume that the dipole-moment vector of a water molecule is colinear with the vector between the mean position of its two H atoms and the position of its O atom as found in the crystal. The direction of the water dipole, estimated in this fashion, should be relatively insensitive to systematic errors in the O—H bond lengths. The orientation of a water dipole with respect to a Ca ion is conveniently expressed in terms of a spherical coordinate system. Fig. 1 shows a water molecule situated in a Cartesian coordinate system with the H—O—H plane placed in the *xz* plane, the water O atom positioned at the origin, and the water dipole coincident with the *z*

Table 1. *References to crystal structure reports from which calcium–water examples are drawn*

$CaCl_2$-$6H_2O$
Agron, P. A. & Busing, W. R. (1969)
Ann. Progr. Rep. ORNL-4437, pp. 118-119.
Chem. Div., Oak Ridge Nat'l Lab.

$CaCrO_4$-H_2O
Bars, O., Le Marouille, J. Y. & Grandjean, D. (1977)
Acta Cryst. B33, 3751-3755.

Ca_3(1,3-Diphosphorylimidazole)$_2$-$12H_2O$
Beard, L. N. & Lenhert, P. G. (1968)
Acta Cryst. B24, 1529-1539.

Ca(Barbital)-$3H_2O$
Berking, B. (1972)
Acta Cryst. B28, 98-113.

Ca(Hydrazinecarboxylate)-H_2O
Braibanti, A., Manotti Lanfredi, A. M.,
Pellinghelli, M. A. & Tiripicchio, A. (1971)
Acta Cryst. B27, 2261-2268.

Ca(Malate)-$2H_2O$
Brändén, C.-I. & Söderberg, B.-O. (1966)
Acta Chem. Scand. 20, 730-738.

Ca(Malonate)-$2H_2O$
Briggman, B. & Oskarsson, Å. (1977)
Acta Cryst. B33, 1900-1906.

Ca_2(Inosine-5'-Monophosphate)$_2$-$13H_2O$
Brown, E. & Bugg, C. E. (1979)
In preparation.

$CaBr_2$(Lactose)-$7H_2O$
Bugg, C. E. (1973)
J. Amer. Chem. Soc. 95, 908-913.

$CaHAsO_4$-$3H_2O$
Catti, M. & Ferraris, G. (1973)
Acta Cryst. B29, 90-96.

$CaSO_4$-$2H_2O$, Gypsum
Cole, W. F. & Lancucki, C. J. (1974)
Acta Cryst. B30, 921-929.

$CaBr_2$(Galactose)-$3H_2O$
Cook, W. J. & Bugg, C. E. (1973a)
J. Amer. Chem. Soc. 95, 6442-6446.

CaBr(Lactobionate)-$4H_2O$
Cook, W. J. & Bugg, C. E. (1973b)
Acta Cryst. B29, 215-222.

$CaCl_2$(Lactose)-$7H_2O$
Cook, W. J. & Bugg, C. E. (1973c)
Acta Cryst. B29, 907-909.

$CaBr_2$(Inositol)-$5H_2O$
Cook, W. J. & Bugg, C. E. (1973d)
Acta Cryst. B29, 2404-2411.

$CaBr_2$(Trehalose)-H_2O
Cook, W. J. & Bugg, C. E. (1973e)
Carbohyd. Res. 31, 265-275.

$CaBr_2$(Fucose)-$3H_2O$
Cook, W. J. & Bugg, C. E. (1975)
Biochim. Biophys. Acta 389, 428-435.

$CaBr_2$(Fructose)-$2H_2O$
Cook, W. J. & Bugg, C. E. (1976)
Acta Cryst. B32, 656-659.

$CaCl_2$(Fructose)-$3H_2O$
Craig, D. C., Stephenson, N. C. &
Stevens, J. D. (1974a).
Cryst. Struct. Comm. 3, 195-199.

$CaCl_2$(Fructose)-$2H_2O$
Craig, D. C., Stephenson, N. C. &
Stevens, J. D. (1974b)
Cryst. Struct. Comm. 3, 277-281.

$CaHPO_4$-$2H_2O$
Curry, N. A. & Jones, D. W. (1971)
J. Chem. Soc. (A), 3725-3729.

$CaCr_2O_7$·$((CH_2)_6N_4)_2$-$7H_2O$
Dahan, F. (1975)
Acta Cryst. B31, 423-426.

$Ca_4Mg(AsB_6O_{11}(OH)_6)_2$-$14H_2O$, Teruggite
Dal Negro, A., Kumbasar, I. & Ungaretti, L. (1973)
Amer. Mineral. 58, 1034-1043.

CaBr(Glucuronate)-$3H_2O$
DeLucas, L., Bugg, C. E., Terzis, A. &
Rivest, R. (1975)
Carbohyd. Res. 41, 19-29.

$CaNa_2(CO_3)_2$-$2H_2O$, Pirssonite
Dickens, B. & Brown, W. E. (1969)
Inorg. Chem. 8, 2093-2103.

$CaNa_2(CO_3)_2$-$5H_2O$, Gaylussite
Dickens, B. & Brown, W. E. (1969)
Inorg. Chem. 8, 2093-2103.

$CaKAsO_4$-$8H_2O$
Dickens, B. & Brown, W. E. (1972)
Acta Cryst. B28, 3056-3065.

Ca(Glutamate)-$3H_2O$
Einspahr, H. & Bugg, C. E. (1974)
Acta Cryst. B30, 1037-1043.

Ca(Glutamate)$_2$-$4H_2O$
Einspahr, H. & Bugg, C. E. (1979a)
In press.

Ca(Asparate)(Ascorbate)-H_2O
Einspahr, H. & Bugg, C. E. (1979b)
In preparation.

CaCl(Glutamate)-H_2O
Einspahr, H., Gartland, G. L. & Bugg,
C. E. (1977)
Acta Cryst. B33, 3385-3390.

$Ca_5(HAsO_4)_2(AsO_4)_2$-$4H_2O$, Sainfeldite
Ferraris, G. & Abbona, F. (1972).
Bull. Soc. Fr. Mineral. Cristallogr. 95, 33-41.

$CaHAsO_4$-$2H_2O$, Pharmacolite
Ferraris, G., Jones, D. W. & Yerkess, J. (1971)
Acta Cryst. B27, 349-354.

$CaHAsO_4$-H_2O, Haidingerite
Ferraris, G., Jones, D. W. & Yerkess, J. (1972)
Acta Cryst. B28, 209-214.

CaBr(Phosphorylcholine)-$4H_2O$
Fontecilla-Camps, J. C., Einspahr, H.
& Bugg, C. E. (1979)
In preparation.

Ca(Garcinate)-$4H_2O$
Glusker, J. P., Minkin, J. A. &
Casciato, C. A. (1971)
Acta Cryst. B27, 1284-1293.

Ca(Hibiscate)-$4H_2O$
Glusker, J. P., Minkin, J. A. & Soule, F. B. (1972)
Acta Cryst. B28, 2499-2505.

CaNa(Galacturonate)$_3$-$6H_2O$
Gould, S. E. B., Gould, R. O., Rees, D. A. &
Scott, W. E. (1975)
J. Chem. Soc. Perkin II, 237-242.

$CaB_3O_4(OH)_3$-H_2O, Colemanite
Hainsworth, F. N. & Petch, H. E. (1966)
Can. J. Phys. 44, 3083-3107.

Ca(Ascorbate)$_2$-$2H_2O$
Hearn, R. A. & Bugg, C. E. (1974)
Acta Cryst. B30, 2705-2711.

CaH_2(Malate)$_2$-$5H_2O$
Hsu, B. & Schlemper, E. O. (1978)
Acta Cryst. B34, 930-932.

CaCu(Acetate)$_4$-$6H_2O$
Langs, D. A. & Hare, C. R. (1967)
Chem. Comm. 890-891.

$CaClNO_3$-$2H_2O$
Leclaire, A. & Borel, M. M. (1978)
Acta Cryst. B34, 902-904.

Alpha-Ca$(NO_3)_2$-$4H_2O$
Leclaire, A. & Monier, J.-C. (1977)
Acta Cryst. B33, 1861-1866.

$Ca_3(SiO_3OH)_2$-$2H_2O$, Afwillite
Malik, K. M. A. & Jeffery, J. W. (1976)
Acta Cryst. B32, 475-480.

$Ca_2P_2O_7$-$2H_2O$
Mandel, N. S. (1975)
Acta Cryst. B31, 1730-1734.

Ca(Glycerate)$_2$-$2H_2O$
Meehan, E. J., Einspahr, H. & Bugg, C. E. (1979)
In press.

$CaCl_2$(1,4,7,10-Tetraoxacyclododecane)-$8H_2O$
North, P. P., Steiner, E. C., Van Remoortere,
F. P. & Boer, F. P. (1976)
Acta Cryst. B32, 370-376.

$CaCl_2$(Allo, Allo-Trehalose)-$5H_2O$
Ollis, J., James, V. J., Angyal, S. J. &
Pojer, P. M. (1978)
Carbohyd. Res. 60, 219-228.

$CaPO_3F$-$2H_2O$
Perloff, A. (1972)
Acta Cryst. B28, 2183-2191.

Ca(Gamma-Carboxyglutamate)-$3H_2O$
Satyshur, K. & Rao, S. T. (1977)
Private communication.

Ca$(H_2PO_4)_2$-H_2O
Schroeder, L. W., Prince, E. & Dickens, B. (1975)
Acta Cryst. B31, 9-12.

CaH(Citrate)-$3H_2O$
Sheldrick, B. (1974)
Acta Cryst. B30, 2056-2057.

Ca(Dipicolinate)-$3H_2O$
Strahs, G. & Dickerson, R. E. (1968)
Acta Cryst. B24, 571-578.

$CaCl_2$(Arabinose)-$4H_2O$
Terzis, A. (1976)
Private communication.

Ca(Thymidylate)-$6H_2O$
Trueblood, K. N., Horn, P. & Luzzati, V. (1961)
Acta Cryst. 14, 965-982.

Ca$(C(CH_3)(OH)(PO_3H)_2)$-$2H_2O$
Uchtman, V. A. (1972)
J. Phys. Chem. 76, 1304-1310.

Ca(Oxydiacetate)-$6H_2O$
Uchtman, V. A. & Oertel, R. P. (1973)
J. Amer. Chem. Soc. 95, 1802-1811.

$CaCl_2$(Glycylglycylglycine)-$3H_2O$
van der Helm, D. & Willoughby, T. V. (1969)
Acta Cryst. B25, 2317-2326.

Ca(Nitrilotriacetate)-$2H_2O$
Whitlow, S. H. (1972)
Acta Cryst. B28, 1914-1919.

Ca(2,4,6,8-Cyclooctatetraene-1,2-dicarboxylate)-$2H_2O$
Wright, D. A., Seff, K. & Shoemaker, D. P. (1972)
J. Cryst. Mol. Struct. 2, 41-51.

axis. R, the radial coordinate in the spherical system, is defined as the Ca––O distance. The angle θ is the acute angle between the water dipole (or z axis) and the Ca––O vector. The angle φ is the acute dihedral angle between (1) the plane defined by the water dipole and the Ca––O vector, and (2) the plane of the water molecule. As defined in the Cartesian system of Fig. 1, φ is the acute (azimuthal) angle between the x axis and the vector from the origin to the projected position of the Ca ion on the xy plane. The angle θ describes the orientation of a Ca ion relative to a water dipole and the angle φ completes the description relative to the water plane.

An additional factor of possible influence in determining calcium–water geometries is the calcium coordination number, which is taken as the number of ligand atoms in the nearest-neighbor sphere about a Ca ion (hydrogen atoms and other electropositive atoms bonded to ligand atoms are not considered in the assignment of coordination numbers). To determine the calcium coordination number in cases where the members of the primary coordination sphere cannot be assigned by inspection, the radial limit is taken at the largest gap in the list (in decreasing order) of reciprocals of distances between Ca and possible ligand atoms (Brunner, 1977), except that no ligand atom with a distance to the Ca ion of less than 2·8 Å was excluded.

We have analyzed for correlations among the parameters θ, φ and R (Ca––O distance); and we have included calcium coordination numbers in the analysis in some cases. We have also looked for correlations involving a parameter that we call d, which is the shorter of the two distances between a Ca ion and the H atoms of a water ligand.

Ca···H *distances*

The large dipole moment of water suggests the possibility that electrostatic repulsions between Ca ions and the H atoms of water molecules might play an important role in determining the permitted combinations of φ and θ values. We are encouraged in this possibility by the success with which somewhat more sophisticated electrostatic considerations (Baur, 1972, 1973) can predict H positions in crystalline hydrates. Qualitatively, this effect can be appreciated from an examination of Fig. 1. For a given value of θ, small values of φ would tend to minimize the distance between the Ca ion and one of the H atoms (the one that lies in the $+x$ direction in Fig. 1). It is expected that, for a given value of θ, only those φ angles above a limiting value are permitted, due to the occurrence of prohibitively short Ca···H distances below this limiting value. In geometrical terms, an actual Ca···H distance will depend on several variables: R, θ and φ; and, assuming a symmetric water molecule, the O–H bond length (r) and the H–O–H intrawater bond angle (2ω). The shorter Ca···H distance (d) is related to these variables by the equation

$$d^2 = R^2 + r^2 + 2Rr(\cos\theta\cos\omega - \sin\theta\sin\omega\cos\varphi). \quad (1)$$

We may apply this equation to estimate limits to the ranges of R, θ and φ, for a given value of d.

Fig. 2 is a compound histogram that shows the distribution of Ca···H distances observed in these crystal structures. The overall distribution has been subdivided to show the distribution of observed d values (hatched): that is, the distribution of the smaller of each pair of observed Ca···H distances. This distribution may be used to estimate the minimum value of d for use in (1). Six of the 149 examples have one or more O–H distances outside a range of 0·6–1·3 Å and are suspected to be examples with systematic errors in O–H bond lengths that seriously affect estimates of Ca···H distances. These examples, shown as speckled areas in Fig. 2, fall at the extremes of the distribution. If these examples are ignored, the observed values of d may be described as normally distributed about a mean of 2·86 Å with a standard deviation of 0·12 Å. The smallest accepted value of d is 2·54 Å, which may be compared to 2·50 Å, the lower border of the 3σ interval

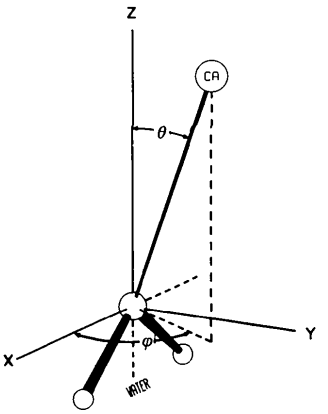

Fig. 1. Spherical and Cartesian coordinate systems for the description of calcium–water geometries.

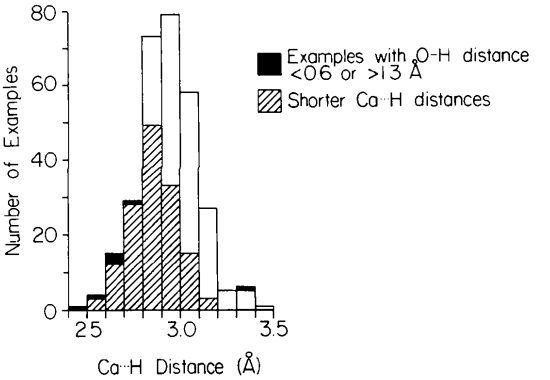

Fig. 2. Histogram showing numbers of examples as a function of Ca···H distance. The distribution of d, the shorter of each pair of Ca···H distances, is shown hatched. Speckled areas indicate examples with Ca···H distances suspected of being affected by extreme values of O–H distance.

about the mean. The Ca···H distances are the only calculated quantities used in this survey that are systematically affected by errors in X-ray-determined H positions. The average is thought to be underestimated by about 0·04–0·05 Å. However, when the five examples with short Ca···H distances are modified by scaling the O—H vectors to 0·96 Å, the shortest resulting Ca···H distance is 2·52 Å, one distance lengthens to near the average value, and the average of the four that remain short is 2·55 Å.

Variation in water-molecule environments

The water molecules that are coordinated to Ca ions in these crystal structures are also involved in a variety of other interactions, some of which are depicted in Fig. 3. In most cases, a water molecule interacts with three species (Fig. 3*a*) such that, in addition to the calcium–water coordination bond, the water molecule uses both H atoms to form hydrogen bonds to suitable acceptor groups. In some cases, the O atom of the water molecule may act as acceptor in an additional H-bond, thereby forming four interactions (Fig. 3*b*). As an alternative fourth interaction, the water molecule may coordinate a second metal ion (as, for example, in Fig. 3*c*). Not illustrated are water molecules forming only two interactions, of which there are six examples, or forming five interactions, of which there are three examples.

We have found it convenient to account for this variability in water-molecule environments, at least qualitatively, by separating the examples according to the number of interactions (H-bonds plus coordination bonds) in which the water molecules are involved, that is, according to water-coordination number. Considering the qualitative effects that the water-coordination number might have on the geometrical parameters θ and φ, as well as the paucity of examples with water-coordination numbers other than three or four, we divide the set of calcium–water examples into only two classes. Those with water-coordination numbers of three or less (representing about two-thirds of the examples) will be referred to as Class 1 examples. Those with water-coordination numbers of four or more will be referred to as Class 2 examples. This classification scheme is more in keeping with the phenomenological approach of Falk & Knop (1973) than the other analyses mentioned previously. One might expect calcium interactions with water molecules of Class 2 to be characterized by θ angles near the tetrahedral value (54·7°) and φ angles of 90°, owing to the stereochemical constraints associated with arranging four or more ligands around a water molecule. On the other hand, the water molecules of Class 1 are not subject to the same degree of steric constraint in selecting an equilibrium configuration. In presenting our results, we distinguish between these two classes of examples where the distinction may be of significance.

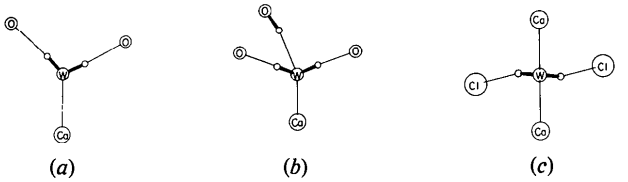

(*a*) (*b*) (*c*)

Fig. 3. The most commonly observed water environments. (*a*) A typical Class 1 example in which the water molecule forms three interactions, (*b*) a Class 2 example in which the water molecule forms four interactions by serving as acceptor of a H bond. (*c*) An alternative to (*b*) in which the water molecule bridges two cations.

Results

Stereo representation of the distribution of calcium–water configurations

Our efforts to analyze the three-dimensional distribution of calcium–water configurations have been aided considerably by stereo representations that convey the major geometrical features. We have plotted

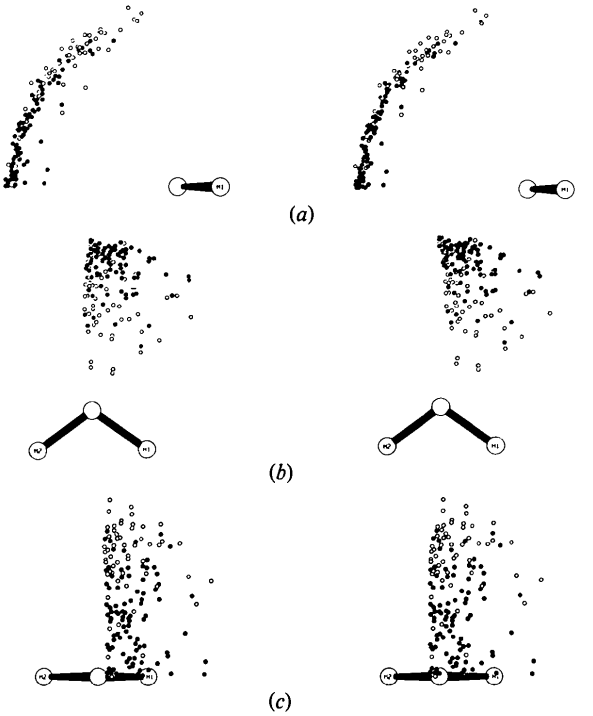

Fig. 4. Stereoplots of the observed distribution of calcium–water configurations. All Ca positions are plotted relative to a single idealized water molecule and are confined to a single octant by invoking the C_{2v} (*mm*2) symmetry of the water molecule. Examples of Class 1 are shown as filled circles, those of Class 2 as open circles. Views (*a*), (*b*) and (*c*) are down the *x*, *y*, and *z* axes of Fig. 1, respectively. In (*c*), some Ca positions have been changed slightly so that all are visible. [These drawings, as well as those of Figs. 1 and 3, were prepared with the aid of *ORTEP* (Johnson, 1965).]

all of the observed Ca positions relative to a single water molecule, and have restricted the Ca positions to a single quadrant of space about the water-oxygen atom by imposing on the distribution the ideal C_{2v} (*mm*2) symmetry of the isolated water molecule. The variety of orientations that Ca ions assume about water molecules in these crystal structures can be seen in the three stereo drawings of Fig. 4. Class 1 examples are shown as filled circles and Class 2 examples are depicted as open circles. In the following analysis, these drawings are used in conjunction with a variety of two-dimensional correlations among the parameters to describe the distribution of observed calcium–water configurations.

Angular distributions

The general distribution as seen in Fig. 4 is characterized by a concentration of examples near the plane that bisects the water molecule. This plane is the locus of φ values of 90°, as defined in Fig. 1. Overall, there is a fairly even distribution of examples at various θ values along a rather narrow segment that lies near the $\varphi = 90°$ plane. However, it is clear that distributions are somewhat different for the two classes of examples. As expected, Class 2 examples (the open circles in Fig. 4) tend to occur at relatively high θ values. On the other hand, Class 1 examples (the filled circles in Fig. 4), tend toward lower θ values.

Graphical representations that summarize the angular distributions depicted in Fig. 4 are given in Figs. 5, 6 and 7. Fig. 5 is a histogram that describes the frequency with which various θ values are observed in these crystal structures. It is evident from this figure that the overall distribution shows no pronounced clustering of examples at any particular value of θ, but instead shows a broad maximum in the 10–50° range. This maximum appears to be composed of two peaks: one in the 10–20° interval, which is mainly attributable to Class 1 examples, and one at about 50°, which is primarily produced by Class 2 examples. The expected tendency of water molecules of Class 2 to bind calcium ions at higher θ values is clearly discernible from Fig. 5.

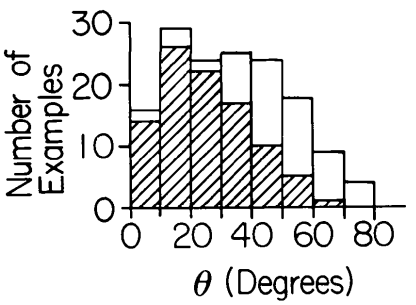

Fig. 5. Histogram showing numbers of examples as a function of θ, the angle between the Ca--O vector and the water-dipole vector. The distribution of Class 1 examples is hatched.

The distribution of φ values is depicted in Fig. 6. As expected from the stereoplots in Fig. 4, there is a tendency for examples to cluster toward φ values of 90°. Some 60% of the examples have φ values in the 70–90° range. The φ distribution falls off very sharply between 90 and 60°, and then flattens to a relatively uniform level, with only one-fourth of the examples occurring below $\varphi = 60°$. In the $\varphi = 0$–60° range, 90% of the examples involve water molecules of Class 1; in the 70–90° range, the distributions of the two classes are approximately equivalent.

Fig. 7 plots the paired values of θ and φ for all the examples in these crystal structures. The observed φ range is broad for small values of θ; below θ values of about 20°, there is no clear preference for any particular φ value. This low-θ region is populated almost exclusively by Class 1 examples (filled circles). As θ increases, the φ range becomes more restricted; for θ angles above 50°, φ values are limited to the range 60–90°.

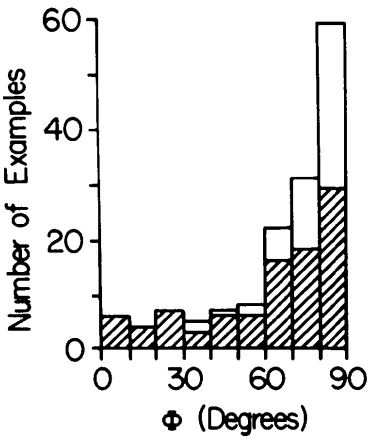

Fig. 6. The φ histogram. The distribution of Class 1 examples is hatched.

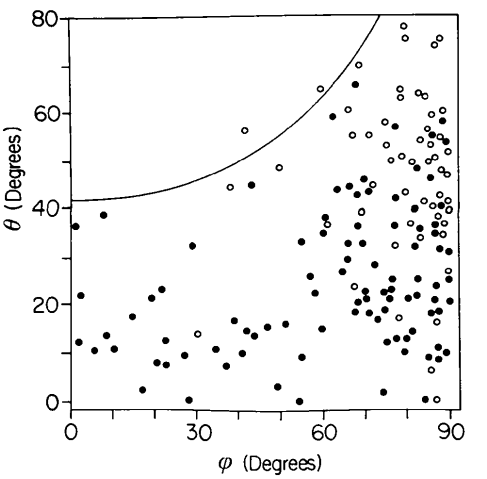

Fig. 7. A plot of paired values of θ and φ, one for each example. Examples of Class 1 are shown as filled circles.

Included in Fig. 7 is a curve [calculated using (1)] of θ,φ combinations that would produce a Ca···H distance of 2·55 Å, assuming a typical value for R of 2·45 Å (for the geometrical parameters of the water molecule, r and ω, we take the average values, 0·96 Å and 54°, respectively, of Ferraris & Franchini-Angela, 1972). For Ca--O distances of 2·45 Å, positions below this curve would correspond to θ,φ combinations that produce Ca···H distances longer than 2·55 Å, whereas points above the curve would correspond to θ,φ combinations that produce Ca···H distances shorter than this limiting value. Curves of similar shape can be produced by assuming other reasonable combinations of d and R. For a given value of d, limiting curves corresponding to longer R values enclose broader areas of the θ,φ plot, while curves for shorter R enclose more restricted areas; for a given value of R, curves for longer d values enclose more restricted areas, while curves for shorter d enclose broader areas. The shape of the curve in Fig. 7 is seen to reflect fairly accurately the confines of the θ,φ distribution. The general shape of this curve has a simple rationale. For small values of θ, Ca···H distances are relatively insensitive to change in φ. On the other hand, the φ range will be restricted at the larger θ values, because as θ increases toward 90°, φ values must also be close to 90° in order to avoid an unusually short distance between the Ca ion and one of the water H atoms.

Lengths of calcium–water coordination bonds

Fig. 8 shows a series of histograms that depict the distribution of distances (R) between the Ca ions and the O atoms of the water molecules. The histogram on the left of Fig. 8 shows the overall distribution for the 149 calcium–water interactions that we examined. The majority of the Ca--O distances lie between 2·3 and 2·5 Å; the average distance is 2·42 Å, which is approximately the sum of the van der Waals radius of O and the ionic radius of Ca. Among these calcium–water examples, we find no Ca--O distance shorter than 2·3 Å; Ca--O distances range out to about 2·7 Å, though few examples occur beyond 2·6 Å. The histograms on the right side of Fig. 8 show individual distributions of Ca--O distances for the various Ca coordination numbers that are observed in these crystal structures. Most of the water molecules occur in sevenfold and eightfold coordination polyhedra, although we have encountered a few examples in sixfold and ninefold patterns. As expected from other studies (see, for example, Fig. 2*b* of Shannon, 1976), the average Ca--O distance varies directly with the calcium coordination number. The breakdown in terms of the two water classes is also shown for each histogram. The histograms reveal that Class 1 examples (hatched) tend to occur more commonly at lower Ca--O distances. Given the previously noted high frequency of Class 1 examples at lower θ values, a possible correlation between R and θ is suggested.

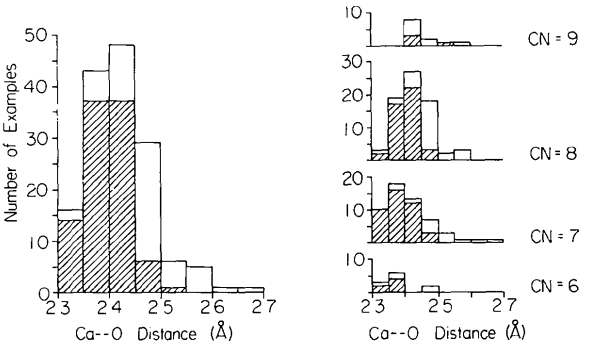

Fig. 8. Histograms showing numbers of examples as a function of R, the Ca--O distance. The four histograms on the right show a breakdown of the overall distribution according to calcium coordination number. Hatched areas show distributions for Class 1 examples.

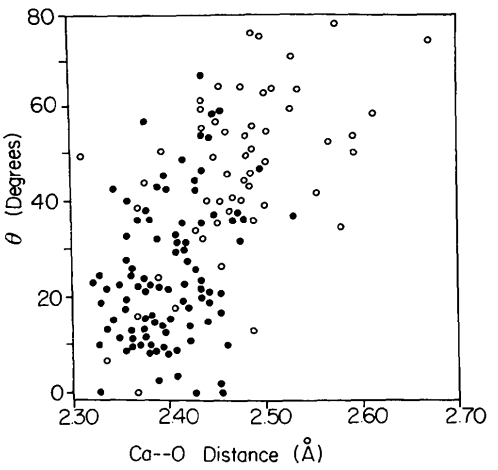

Fig. 9. A plot of paired values of θ and R (Ca--O distance), one for each example. Examples of Class 1 are shown as filled circles.

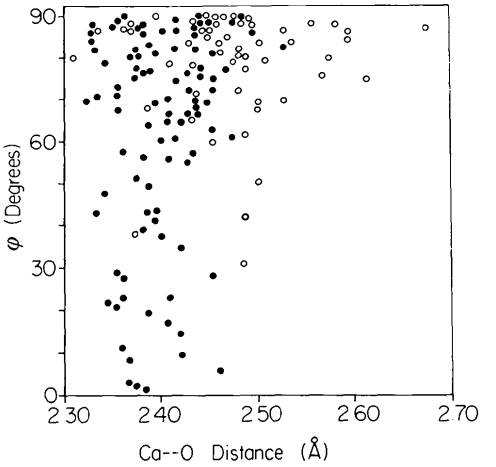

Fig. 10. A plot of paired values of φ and R (Ca--O distance), one for each example. Examples of Class 1 are shown as filled circles.

Fig. 9, a scatter plot of paired values of R and θ for all examples in these crystal structures, shows the R,θ correlation directly. It is apparent that the Ca--O distance tends to increase as θ increases. Though the scatter of examples is great, R is nearer the short end of its range when θ is small, and is nearer the outer end of its range when θ is large. The segregation of the two water classes is clearly seen in Fig. 9. Examples of Class 1 (filled circles) dominate the lower R,θ region and tail off toward higher R,θ values; Class 2 examples (open circles) have a somewhat more diffuse distribution, but predominate in higher R,θ regions.

Fig. 10 shows a scatter plot of φ *versus* Ca--O distance. The major features of Fig. 10 are predictable from the θ,φ and the θ,R plots that are depicted in Figs. 7 and 9. Lower values of φ, which are only found in low θ ranges, correspond to shorter Ca--O distances; values of φ near 90°, which are found over a wide range of θ values, cover the complete range of possible Ca--O distances. Shorter values of R, corresponding to smaller values of θ, cover the complete range of φ values. Distributions of the two water classes follow the general patterns suggested by Figs. 7 and 9.

Discussion

Several features of the observed distribution of calcium–water configurations deserve particular emphasis. One is the pronounced tendency for Ca ions to lie near the plane that bisects the water molecule. The high density of examples in this region, which corresponds roughly to the $\varphi = 90°$ region of our spherical coordinate system, can be seen in the stereoplots of Fig. 4, and is further underscored by the φ-distribution histogram (Fig. 6). Most of the examples lie within a relatively narrow band that borders on the $\varphi = 90°$ plane. While several examples show large deviations from $\varphi = 90°$ (Fig. 6), the majority of these have low θ values and lie within the band in the region near the plane of the water molecule (Fig. 4*c*). It should be noted that, apart from the tail-off at high θ, the density of examples is fairly even within this band; no segment of the band stands out as having a markedly higher population of examples than other segments. Thus our results provide no indication that any particular θ value is preferred in these crystal structures.

A second feature that deserves emphasis is the correlation between Ca--O distance and θ. This correlation is not readily observable in the stereoplots of Fig. 4 because the differences in individual Ca--O distances are relatively small. It is in Fig. 9, however, that this relationship becomes apparent. Although the scatter of examples is large, the trend of short R at low θ to long R at high θ is evident, and the majority of examples lie in a band that runs from about 2·3–2·4 Å at low θ to 2·45–2·55 Å at high θ.

A third noteworthy feature of the observed distribution is the result of distinguishing two classes of calcium–water examples according to the number of bonding interactions in which the water molecule is involved. A segregation of the two classes on the basis of one or more geometrical parameters is seen in all of our representations of the distribution of calcium–water geometries (Figs. 4–10). Examples with water molecules that form two or three interactions (*i.e.* Class 1 examples) occur more commonly at shorter Ca--O distances and lower θ values, but cover the complete range of φ values. Examples with water molecules that form four or five interactions (*i.e.* Class 2 examples) occur more commonly at longer Ca--O distances, higher θ, and φ near 90°. The separation between the classes is not abrupt in any of the representations; the two classes are seen to intergrade smoothly, and regions of overlap between the two classes do not show reduced population densities.

The results of our analysis point to significant restrictions on the range of calcium–water geometries and indicate that, even for a relatively uncomplicated ligand such as water, geometrical preferences of the ligand influence coordination interactions with the Ca ion. Of course, a number of complicating factors affect the distribution of calcium–water geometries observed in these crystal structures. Although we have attempted to account in part for the variation in water environments by classifying examples according to the number of water interactions, the range of crystallographic environments is large and a number of important environmental factors remain unanalyzed. Furthermore, errors in hydrogen positions are an experimental factor that undoubtedly affects the distribution of configurations. Nevertheless, the major features of the distribution appear to be consistent with those that might be expected for calcium–water interactions in other, non-crystalline environments.

While our observations may be rationalized by a number of qualitative models, we feel that the major features can be adequately accounted for in terms of simple electrostatic factors, which involve an attractive interaction between the Ca ion and the O atom of the polar water molecule, coupled with repulsive interactions between the Ca ion and the water H atoms. We have described earlier how one might explain the concentration of examples near the $\varphi = 90°$ plane in terms of Ca···H repulsions. From simple electrostatic considerations, we would expect that the most stable configuration for an isolated calcium–water complex (in which the water molecule is bound only to the Ca ion) places the Ca ion colinear with the dipole-moment vector of the water molecule (*i.e.* $\theta = 0°$); however, our actual distribution (Fig. 4) does not show a significant preference for this configuration in crystal structures. This discrepancy may be attributable to fundamental environmental differences between isolated and crystal-

line complexes, since most of the water molecules in these crystal structures are bound to two or more species in addition to the Ca ion. The apparent relationship between θ and Ca--O distance (Fig. 9) indicates that the shorter (*i.e.* stronger) calcium–water interactions are those with configurations where the Ca ion is more nearly colinear with the water dipole. The segregation of Class 1 and Class 2 examples in Fig. 9 lends support to this interpretation: Class 1 examples, which have water molecules that are subject to fewer competing interactions than those from Class 2 examples, show shorter Ca--O distances and lower θ values. This trend, when extrapolated to the isolated system, suggests a preferred configuration which is consistent with that predicted by simple electrostatic considerations.

We thank Drs Craig, Stephenson & Stevens; Schemper; Langs; Angyal; Satyshur & Rao; Sheldrick; and Terzis for providing data prior to publication. We also gratefully acknowledge the assistance provided by Drs Ferraris and Leclaire in alerting us to the existence of structure reports that are included in this study.

In addition, we thank Mrs Mary Ann Jones for assistance with data processing and preparation of the drawings and manuscript. This work was supported by NIH grants CA-12159, CA-13148 and DE-02670.

References*

BAUR, W. H. (1972). *Acta Cryst.* B**28**, 1456–1465.
BAUR, W. H. (1973). *Acta Cryst.* B**29**, 139–140.
BRUNNER, G. O. (1977). *Acta Cryst.* A**33**, 226–227.
CHIDAMBARAM, R., SEQUEIRA, A. & SIKKA, S. K. (1964). *J. Chem. Phys.* **41**, 3616–3622.
DIERCKSEN, G. H. F., KRAEMER, W. P. & ROOS, B. O. (1975). *Theor. Chim. Acta*, **36**, 249–274.
FALK, M. & KNOP, O. (1973). In *Water: A Comprehensive Treatise*, edited by F. FRANKS, Vol. II. New York: Plenum.
FERRARIS, G. & FRANCHINI-ANGELA, M. (1972). *Acta Cryst.* B**28**, 3572–3583.
FRIEDMAN, H. L. & LEWIS, L. (1976). *J. Solution Chem.* **5**, 445–455.
HAMILTON, W. C. & IBERS, J. A. (1968). *Hydrogen Bonding in Solids*, pp. 204–208. New York: Benjamin.
JOHNSON, C. K. (1965). *ORTEP*. Report ORNL-3794, revised. Oak Ridge National Laboratory, Oak Ridge, Tennessee.
KOLLMAN, P. A. & KUNTZ, I. D. (1972). *J. Am. Chem. Soc.* **94**, 9236–9237.
PERAHIA, D., PULLMAN, A. & PULLMAN, B. (1976). *Theor. Chim. Acta*, **42**, 23–31.
SHANNON, R. D. (1976). *Acta Cryst.* A**32**, 751–767.

* See also Table 1.

Acta Cryst. (1980). B**36**, 271–275

On the Geometry of Urea–Cation Bonding in Crystalline Urea Adducts

BY ŁUKASZ LEBIODA

Institute of Chemistry, Jagiellonian University, ul. Karasia 3, 30-060 *Kraków, Poland*

(*Received* 9 *January* 1979; *accepted* 8 *August* 1979)

Abstract

A survey of 26 crystal structures of urea adducts has revealed that there are systematic features in urea–cation bonding. It has been found that in complexes with monovalent cations urea coordinates to two cations. In complexes with divalent cations urea shows a preference to bond to only one cation, in the plane of the molecule, with an M^{2+}–C=O angle of about 130–140°, rather than along the dipole-moment direction. The preferred geometry is the same for transition- and non-transition-metal cations.

Introduction

A systematic survey of crystalline urea adducts formed with a large variety of inorganic salts was undertaken as a part of a study of cation bonding to the amide group. The rationale behind this kind of study is that much information of chemical interest is imbedded in crystal structures, which represent minimum-energy arrangements. Little information about intermolecular interactions can be extracted from a single structure alone; however, certain trends are apparent if sufficient structural data are taken into account. Although a great deal is known about how cations bond to ligands, relatively little work has been carried out to determine how a ligand bonds to cations.

The aim of this work was to establish the preferred geometry of urea–cation bonding. The structural relationships in cation–urea complexes can be of some relevance in a discussion of interactions between cations and amides or peptide groups, especially in the *cis*-planar conformation which is often found in oligopeptides, which act as ion carriers (Karle, 1975).

0567-7408/80/020271-05$01.00